International Journal of Thermophysics, Vol. 23, No. 2, March 2002 (© 2002)

The Thermal Conductivity, Thermal Diffusivity, and Specific Heat of Liquid *n*-Pentane[1]

L. Sun,[2] J. E. S. Venart,[2, 3] and R. C. Prasad[4]

Received August 20, 2001

The thermal conductivity and thermal diffusivity of liquid *n*-pentane have been measured over the temperature range from 293 to 428 K at pressures from 3.5 to 35 MPa using a transient hot-wire instrument. It was determined that the results were influenced by fluid thermal radiation, and a new expression for this effect is presented. The uncertainty of the experimental results is estimated to be better than $\pm 0.5\%$ for thermal conductivity and $\pm 2\%$ for thermal diffusivity. The results, corrected for fluid thermal radiation, are correlated as functions of temperature and density with a maximum uncertainty of $\pm 2\%$ for thermal conductivity and $\pm 4\%$ for thermal diffusivity. Derived values of the isobaric specific heat are also given.

KEY WORDS: *n*-pentane; thermal radiation; thermal conductivity; thermal diffusivity; transient hot-wire technique; specific heat.

1. INTRODUCTION

Pentane is an important component of natural gases and some artificial fuels. The fluid is also considered a potential working substance for refrigeration cycles. The thermal conductivity and thermal diffusivity data for *n*-pentane appear limited; there is only one significant data set for the thermal conductivity of vapor at ambient pressure from 313 to 573 K [1]

[1] Parts of this paper presented at the Fourteenth Symposium on Thermophysical Properties, June 25–30, 2000, Boulder, Colorado, U.S.A.

[2] Department of Mechanical Engineering, University of New Brunswick, P.O. Box 4400, Fredericton, New Brunswick, Canada E3B 5A3.

[3] To whom correspondence should be addressed. E-mail: jvenart@unb.ca.

[4] Department of Engineering, University of New Brunswick, Saint John, New Brunswick, Canada E2L 4L5.

0195-928X/02/0300-0391/0 © 2002 Plenum Publishing Corporation

—and two for liquid from 273 to 323 K [2, 3]. No data for thermal diffusivity can be found.

In this paper, absolute measurements of the thermal conductivity and thermal diffusivity of liquid *n*-pentane are presented in the temperature range from 296 to 428 K at pressures to 34 MPa. The data are correlated with density. The precision and reproducibility of the instrument are estimated to be better than $\pm 0.25\%$ for thermal conductivity and $\pm 1\%$ for thermal diffusivity. The measurements, corrected for fluid radiation, are estimated to have an uncertainty of $\pm 0.5\%$ for thermal conductivity and $\pm 2\%$ for thermal diffusivity. Derived values of isobaric specific heat are considered accurate to $\pm 2.5\%$ though this is dependent upon the equation of state utilized.

2. METHOD

The transient hot-wire method is widely accepted as a primary instrument for accurate measurements of fluid thermal conductivity on a wide variety of fluids. Though theoretically feasible, practical simultaneous use for thermal diffusivity measurements has been limited due to the lack of reproducibility and a dependence of the results on the power employed.

The working equation for thermal conductivity is based on the transient solution of Fourier's law for an infinite line source [4, 5]. The ideal temperature rise of the fluid, at the wire–fluid interface, $r = a$, at time t is

$$\Delta T = \frac{q}{4\pi\lambda(\rho, T)} \ln \frac{4\alpha t}{a^2 C} \tag{1}$$

where

$$\Delta T = \Delta T_w + \Sigma\, \delta T_i \tag{2}$$

and $\Sigma\, \delta T_i$ are appropriate corrections to the measured temperature rise, ΔT_w, q is the power per unit length applied to the wire, λ is the thermal conductivity, $\alpha = \lambda/(\rho C_p)$ is the thermal diffusivity, ρ is the density, and C_p is the isobaric heat capacity (all of the fluid), with $C = 1.781\cdots$ the exponential of Euler's constant. One of the necessary corrections to ΔT_w accounts for thermal radiation, δT_{rad}.

For fluids that absorb radiation, Nieto de Castro and fellow workers [6–8] have shown that the dominant correction term in the heat flux gradient arises from the emission of radiation by the heated fluid [9]. These considerations allowed them to derive an approximate analytic solution to the applicable energy equation. In this result, however, the wire itself was

regarded as part of the fluid since the inner boundary condition was considered to be $r = 0$ and not $r = a$. To eliminate this inaccuracy and check the validity of their correction, a new solution is obtained here using the inner boundary condition,, $r = a$, and taking the thermophysical properties of the wire into account.

This solution can be written (Appendix)

$$\Delta T(a, t) = \Delta T_w(a, t) + \frac{f a^2 q \lambda_1 \alpha_2}{8\pi\lambda_2^2 \alpha_1} \ln \frac{4\alpha_2 t}{a^2 C} + \frac{q f a^2}{16\pi\lambda_2}\left(\frac{-\pi^2}{6} + \ln^2 \frac{4\alpha_2 t}{a^2 C}\right) - \frac{q f \alpha_2 t}{4\pi\lambda_2} - \frac{q f a^2}{8\pi\lambda_2} \tag{3}$$

where

$$f = \frac{B}{\alpha_2} \qquad \text{and} \qquad B = \frac{16 K n^2 \sigma T_0^2}{(\rho C p)_2} \tag{4}$$

The temperature rise ΔT_w represents the corrected measured temperature difference (aside from fluid radiation) and ΔT the ideal, and now radiation-corrected, temperature difference. K is the mean absorption coefficient and n is the refractive index of the fluid (both considered temperature independent), σ is the Stephan–Boltzmann constant, and the subscripts 1 and 2 denote the wire and the fluid, respectively. This result yields corrections to both the thermal conductivity and the thermal diffusivity that are slightly different from the results of Nieto de Castro et al. [7] (Appendix).

In reducing the transient data to obtain the corrected temperature difference, and hence the thermal conductivity and thermal diffusivity, one must also consider the influence of the temperature variation of the various thermal properties as the wire temperature changes. This may be expressed as [5]

$$\Delta T = -\frac{1}{2}\chi\, \Delta T^2 + \frac{q}{4\pi\lambda(\rho, T_0)} \ln \frac{4\alpha t}{a^2 C} + \left(\frac{q}{4\pi\lambda}\right)^2 (\chi - \phi) \ln 4 \tag{5}$$

and thus the reference temperature for the measured thermal conductivity can be stated

$$T_r = T_0 + \tfrac{1}{2}[\Delta T(t_1) + \Delta T(t_2)] \tag{6}$$

and no correction for changes with temperature are necessary, despite the fact that over the measurement period (typically 1 to 3 s and ΔT's of 1 to 8 K),

the properties may change significantly. Here $\Delta T(t_1)$ and $\Delta T(t_2)$ represent the temperature rises at the start, t_1, and end, t_2, of the measurement.

Measurements of the thermal diffusivity of the fluid are often attempted (e.g., Refs. 8 and 10) from the same measurements as the thermal conductivity through the use of Eq. (1) in the form

$$\alpha = \frac{a^2 C}{4t'} \exp[4\pi\lambda(P, T_r)\, \Delta T(a, t')/q] \tag{7}$$

To obtain accurate values of this property, however, the temperature coefficient of the thermal conductivity, χ, must be known since over the usual 1-s measurement period the temperature varies by typically 1 to 5 K. This variation may be evaluated from a series of measurements at different wire powers to obtain values of λ at several reference states via Eq. (6). The data may now be fit as a linear function of temperature $\lambda = \lambda_0(1 + \chi\, \Delta T)$. The thermal diffusivity should now be obtained via the slope of the linear fit of ΔT versus q with Eq. (5) at T_0. Then the temperature rise after correcting for the influence of χ can be written

$$\Delta T' = \Delta T + \frac{1}{2}\chi\, \Delta T^2 = \frac{q}{4\pi\lambda(\rho, T_0)} \ln \frac{4\alpha t}{a^2 C} + \left(\frac{q}{4\pi\lambda}\right)^2 (\chi - \phi) \ln 4 \tag{8}$$

The thermal diffusivity must now be obtained via the intercept and slope of the linear fit of ΔT versus q with Eq. (8) at T_0. However, despite this correction a variation in the determined thermal diffusivity values as a function of wire power can usually be observed [8, 11]. This behavior can only be explained through there being an apparent "zero" time, and hence equilibrium temperature, residual bridge imbalance temperature difference despite best attempts at bridge balance. This value must now be determined and the thermal diffusivity results corrected via the relationship between the temperature rise of the hot wire at some determined time versus applied power [11, 12]. Though small (1 to 10 mK), the correction is essential to achieve good reproducibility and accuracy in α.

3. EXPERIMENTAL

A transient hot-wire instrument was modified to allow improved measurements of both thermal conductivity and thermal diffusivity [11–13]. Two wires, each of different length, were used for end effect compensation. The wires were calibrated over the temperature and pressure range of measurement in situ. The wire specifications and calibration coefficients are

Table I. Wire and Test Fluid Specifications

(a) Calibration equation: $R = a_0 + a_1 T + a_2 T^2 + bP$ [T(°C), P (MPa)]		
(b) Wire specification and calibration coefficients; long and short wires		
Purity (%)	99.999	99.999
Lenght (m)	8.549×10^{-2}	3.395×10^{-2}
Diameter (μm)	13.06	13.06
a_0	63.41856	24.90227
a_1	0.250988	0.100879
a_2	-1.11633×10^{-4}	-4.27329×10^{-5}
b	-2.12334×10^{-3}	-5.29280×10^{-4}
(c) Test fluid: *n*-pentane; $M = 72.186$, 99.5% pure		
T_{cr} (469.87 K)	P_{cr} (3.374 MPa)	ρ_{cr} (232 kg·m^{-3})

given in Table I. The wire diameter was obtained from SEM photographs, while the length was measured with a cathetometer with resolutions of ± 0.05 and ± 25 μm, respectively. The principle of the measurement, as well as details of apparatus are described elsewhere [11, 12], so only the major instrument components are discussed here.

The measurement bridge used is shown in Fig. 1 [12]. Here the HP3497A is a data acquisition/control unit, the HP6625A is a dc power supply, the HP3458A is an integrating voltmeter which provides integration for times of 0 to 16667 ms, the HP3437A is an external trigger unit, and C-MOS is a digital switch used to switch from the "dummy" to the "measurement" circuit. The HP3497A unit is used both to provide constant currents of 1, 0.1, and 0.01 mA when calibrating the wires and balancing the bridge, and also as an integrating voltmeter with integration times of 0.167, 1.67, and 16.67 ms along with sets of digital switches used to monitor the circuit, under computer control, during the preliminary balancing as well as during the measurement process. The HP6625A provides a high-stability fast response power supply with 0 to 16 V output to heat the wires.

As indicated the HP3497A unit is used for several purposes. First, it provides the voltmeter to measure the voltage across the standard resistance, R_{st}, to determine the current through the wires. Second, it also provides a 1-mA current used when balancing the bridge. Finally, it provides the digital switches used to connect and disconnect different parts of the circuit. The HP3458A is used to measure the transient imbalance of the bridge introduced by the temperature change of the hot wires and the voltages in every branch of the bridge. The methods of determining and

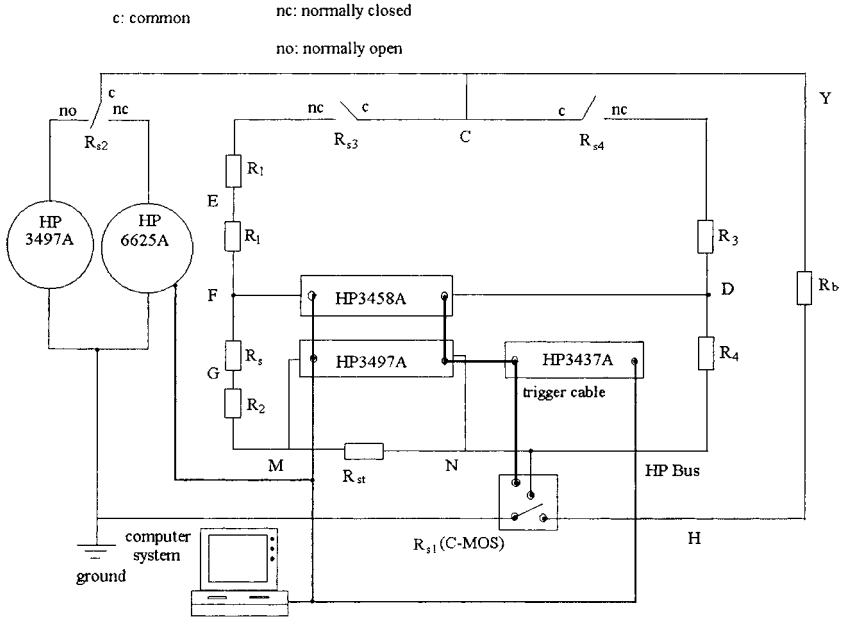

Fig. 1. Transient line source thermal conductivity and thermal diffusivity bridge and associated instrumentation.

correcting the bridge balance and the effective "zero"-time residual bridge imbalance temperatures are given elsewhere [11, 12].

The HP3437A is used to trigger the HP3497A, HP3458A, and C-MOS switch to connect circuit components and to begin simultaneous measurements of both the current and the voltage across the bridge elements.

4. RESULTS AND DISCUSSION

The thermal conductivity and thermal diffusivity of *n*-pentane were measured along isotherms at six nominal temperatures, 296, 317, 340, 375, 401, and 428 K, at pressures from 3.5 to 35 MPa. The temperature, pressure, density, and measured thermal conductivity as well as the equilibrium or thermostat reference state (temperature, pressure, density, thermal conductivity, and thermal diffusivity) values are given in Table II. The density values in the table were obtained using the of equation of state from Ref. 14.

It was found that significant fluid radiation effects were present and thus values of the radiation correction parameter B [Eq. (4)] necessary to make the $\Delta T \sim \ln(t)$ function linear are also tabulated. These values, though small, significantly influence the data as will now be discussed.

Table II. Thermal Conductivity and Thermal Diffusivity of *n*-Pentane

ID No.	T (K)	P (kPa)	ρ ($kg \cdot m^{-3}$)	q ($W \cdot m^{-1}$)	λ ($W \cdot m^{-1} \cdot K^{-1}$)	α ($10^{-8} m^2 \cdot s^{-1}$)	C_p ($J \cdot kg^{-1} \cdot K^{-1}$)	B (s^{-1})
	296.50	**3,535**	**626.73**		**0.1123**	**7.760**	**2,309**	
P20_05A3	297.15	3,535	626.100	0.13438	0.1122			0.005
P20_05A4	297.69	3,535	625.597	0.23840	0.1120			0.005
P20_05A5	298.39	3,535	624.930	0.37199	0.1117			0.005
P20_05A6	299.25	3,535	624.111	0.53418	0.1114			0.005
P20_05A7	300.23	3,535	623.175	0.72425	0.1112			0.005
P20_05A8	301.54	3,535	621.922	0.94225	0.1107			0.005
	296.29	**7,081**	**631.05**		**0.1148**	**7.995**	**2,275**	
P20_10A2	296.90	7,081	630.493	0.05979	0.1145			0.005
P20_10A3	297.43	7,081	630.008	0.13448	0.1143			0.005
P20_10A4	298.15	7,081	629.348	0.23872	0.1140			0.006
P20_10A5	298.99	7,081	628.557	0.37159	0.1137			0.007
P20_10A6	300.06	7,081	627.594	0.53360	0.1133			0.005
P20_10A7	301.08	7,081	626.655	0.72508	0.1130			0.007
	296.71	**13,218**	**637.28**		**0.1179**	**8.122**	**2,278**	
P20_20A3	297.25	13,218	636.812	0.13441	0.1178			0.005
P20_20A4	297.83	13,218	636.310	0.23870	0.1176			0.006
P20_20A5	298.50	13,218	635.730	0.37178	0.1173			0.005
P20_20A6	299.31	13,218	635.028	0.53390	0.1170			0.005
P20_20A7	300.33	13,218	634.143	0.72400	0.1167			0.005
P20_20A8	301.44	13,218	633.179	0.94192	0.1164			0.005
	297.10	**20,413**	**643.99**		**0.1216**	**8.322**	**2,269**	
P20_30A3	297.54	20,413	643.632	0.13445	0.1214			0.005
P20_30A4	298.12	20,413	643.158	0.23856	0.1213			0.006
P20_30A5	298.82	20,413	642.586	0.37205	0.1210			0.005
P20_30A6	299.71	20,413	641.857	0.53509	0.1207			0.005
P20_30A7	300.62	20,413	641.112	0.72564	0.1203			0.006
P20_30A8	301.67	20,413	640.252	0.94450	0.1200			0.005
	297.23	**27,719**	**650.414**		**0.1251**	**8.488**	**2,266**	
P20_40A3	297.79	27,719	649.978	0.13457	0.1249			0.005
P20_40A4	298.34	27.719	649.550	0.23885	0.1248			0.005
P20_40A5	298.96	27,719	649.068	0.37245	0.1245			0.005
P20_40A6	299.72	27,719	648.476	0.53465	0.1243			0.005
P20_40A7	300.65	27,719	647.753	0.72525	0.1240			0.005
P20_40A8	301.63	27,719	646.990	0.94409	0.1237			0.005
	297.27	**34,608**	**656.06**		**0.1284**	**8.683**	**2,254**	
P20_50A3	297.91	34,608	655.584	0.13461	0.1282			0.005
P20_50A4	298.39	34,608	655.226	0.23906	0.1281			0.006
P20_50A5	298.97	34,608	654.793	0.37271	0.1277			0.005
P20_50A6	299.71	34,608	654.241	0.53524	0.1275			0.005
P20_50A7	300.57	34,608	653.599	0.72607	0.1273			0.005
P20_50A8	301.56	34,608	652.860	0.94381	0.1270			0.005

Table II. *(Continued)*

ID No.	T (K)	P (kPa)	ρ ($kg \cdot m^{-3}$)	q ($W \cdot m^{-1}$)	λ ($W \cdot m^{-1} \cdot K^{-1}$)	α ($10^{-8} m^2 \cdot s^{-1}$)	C_p ($J \cdot kg^{-1} \cdot K^{-1}$)	B (s^{-1})
	317.54	**3,372**	**606.09**		**0.1040**	**7.142**	**2,403**	
P45_05A3	318.27	3,372	605.358	0.13298	0.1038			0.012
P45_05A4	318.88	3,372	604.750	0.23598	0.1036			0.012
P45_05A5	319.60	3,372	604.030	0.36810	0.1034			0.012
P45_05A6	320.42	3,372	603.209	0.52879	0.1031			0.012
P45_05A7	321.36	3,372	602.265	0.71734	0.1029			0.012
P45_05A8	322.49	3,372	601.128	0.93322	0.1026			0.012
	317.56	**6,795**	**610.87**		**0.1063**	**7.330**	**2,374**	
P45_10A3	318.19	6,795	610.274	0.13285	0.1061			0.012
P45_10A4	318.81	6,795	609.683	0.23563	0.1059			0.012
P45_10A5	319.53	6,795	608.995	0.36744	0.1058			0.012
P45_10A6	320.36	6,795	608.201	0.52815	0.1054			0.012
P45_10A7	321.42	6,795	607.186	0.71675	0.1051			0.012
P45_10A8	322.48	6,795	606.168	0.93309	0.1048			0.012
	317.14	**13,620**	**619.89**		**0.1106**	**7.615**	**2,343**	
P45_20A3	317.87	13,620	619.245	0.13252	0.1105			0.01
P45_20A4	318.16	13,620	618.989	0.23530	0.1103			0.01
O45_20A5	318.92	13,620	618.317	0.36733	0.1100			0.01
P45_20A6	319.87	13,620	617.477	0.52812	0.1097			0.01
P45_20A7	320.98	13,620	616.494	0.71729	0.1095			0.012
P45_20A8	322.11	13,620	615.492	0.93263	0.1091			0.012
	317.42	**20,463**	**627.33**		**0.1143**	**7.841**	**2,324**	
P45_30A3	318.02	20,463	626.829	0.13276	0.1141			0.01
P45_30A4	318.60	20,463	626.349	0.23559	0.1140			0.01
P45_30A5	319.28	20,463	625.785	0.36749	0.1138			0.01
P45_30A6	320.06	20,463	625.137	0.52788	0.1134			0.01
P45_30A7	321.03	20,463	624.332	0.71622	0.1132			0.01
P45_30A8	322.10	20,463	623.443	0.93245	0.1129			0.01
	317.44	**27,351**	**634.29**		**0.1179**	**8.037**	**2,313**	
P45_40A3	318.04	27,351	633.823	0.13271	0.1177			0.01
P45_40A4	318.59	27,351	633.391	0.23554	0.1176			0.01
P45_40A5	319.23	27,351	632.888	0.36741	0.1174			0.01
P45_40A6	320.03	27,351	632.260	0.52768	0.1172			0.01
P45_40A7	320.97	27,351	631.521	0.71619	0.1170			0.011
P45_40A8	321.97	27,351	630.735	0.93210	0.1167			0.01
	317.50	**34,052**	**640.47**		**0.1212**	**8.230**	**2,299**	
P40_50A3	318.03	34,052	640.069	0.13271	0.1210			0.01
P40_50A4	318.59	34,052	639.650	0.23534	0.1209			0.01
P40_50A5	319.24	34,052	639.162	0.36707	0.1207			0.01
P40_50A6	320.03	34,052	638.570	0.52744	0.1205			0.01
P40_50A7	320.94	34,052	637.887	0.71565	0.1203			0.011
P40_50A8	321.98	34,052	637.107	0.93178	0.1200			0.011

Table II. *(Continued)*

ID No.	T (K)	P (kPa)	ρ ($kg \cdot m^{-3}$)	q ($W \cdot m^{-1}$)	λ ($W \cdot m^{-1} \cdot K^{-1}$)	α ($10^{-8} m^2 \cdot s^{-1}$)	C_p ($J \cdot kg^{-1} \cdot K^{-1}$)	B (s^{-1})
	340.99	**3,396**	**582.02**		**0.09578**	**6.671**	**2,467**	
P70_05A3	341.85	3,396	581.108	0.14312	0.09554			0.022
P70_05A4	342.50	3,396	580.413	0.25406	0.09558			0.022
P70_05A6	344.27	3,396	578.515	0.56935	0.09496			0.022
P70_05A7	345.35	3,396	577.350	0.77254	0.09476			0.02
P70_05A8	346.77	3,396	575.813	1.00617	0.09458			0.02
	340.97	**6,790**	**588.01**		**0.09822**	**6.831**	**2,445**	
P70_10A3	341.14	6,790	587.839	0.14307	0.09808			0.02
P70_10A4	341.84	6,790	587.135	0.25392	0.09797			0.02
P70_10A5	343.23	6,790	585.734	0.39577	0.09787			0.02
P70_10A6	344.15	6,790	584.804	0.56875	0.09762			0.02
P70_10A7	345.26	6,790	583.679	0.77253	0.09746			0.02
P70_10A8	346.56	6,790	582.358	1.00631	0.09727			0.02
	340.56	**13,687**	**599.00**		**0.1029**	**7.001**	**2,454**	
P70_20A3	341.15	13,687	598.460	0.14274	0.1027			0.015
P70_20A4	341.96	13,687	597.721	0.25344	0.1026			0.015
P70_20A5	342.82	13,687	596.935	0.39509	0.1025			0.016
P70_20A6	343.68	13,687	596.149	0.56773	0.1022			0.016
P70_20A7	344.63	13,687	595.279	0.76993	0.1021			0.02
P70_20A8	345.82	13,687	594.186	1.00200	0.1019			0.02
	340.42	**20,500**	**608.14**		**0.1067**	**7.340**	**2,390**	
P70_30A3	340.55	20,500	608.027	0.14262	0.1066			0.015
P70_30A4	341.39	20,500	607.317	0.25310	0.1065			0.018
P70_30A5	342.60	20,500	606.294	0.39522	0.1065			0.018
P70_30A6	343.51	20,500	605.523	0.56780	0.1064			0.018
P70_30A7	344.55	20,500	604.642	0.77011	0.1062			0.018
P70_30A8	346.71	20,500	602.808	1.00128	0.1061			0.018
	340.62	**27,332**	**615.99**		**0.1105**	**7.498**	**2,392**	
P70_40A3	341.37	27,332	615.392	0.14266	0.1104			0.015
P70_40A4	341.89	27,332	614.988	0.25317	0.1103			0.018
P70_40A5	342.65	27,332	614.375	0.39527	0.1102			0.016
P70_40A6	343.56	27,332	613.652	0.56828	0.1101			0.018
P70_40A7	344.62	27,332	612.810	0.77096	0.1099			0.018
P70_40A8	345.73	27,332	611.927	1.00426	0.1098			0.018
	340.79	**34,211**	**623.14**		**0.1140**	**7.792**	**2,348**	
P70_10A3	341.39	34,211	622.684	0.14288	0.1139			0.012
P70_10A4	342.00	34,211	622.226	0.25355	0.1139			0.015
P70_10A5	342.76	34,211	621.654	0.39562	0.1136			0.015
P70_10A6	343.66	34,211	620.977	0.56850	0.1136			0.015
P70_10A7	344.70	34,211	620.195	0.77160	0.1135			0.015
P70_10A8	345.84	34,211	619.337	1.00488	0.1133			0.015
	376.02	**3,369**	**542.05**		**0.08625**	**5.778**	**2,754**	
P10_05A2	376.49	3,369	541.472	0.07035	0.08614			0.03

Table II. *(Continued)*

ID No.	T (K)	P (kPa)	ρ ($kg \cdot m^{-3}$)	q ($W \cdot m^{-1}$)	λ ($W \cdot m^{-1} \cdot K^{-1}$)	α ($10^{-8} m^2 \cdot s^{-1}$)	C_p ($J \cdot kg^{-1} \cdot K^{-1}$)	B (s^{-1})
P10_05A3	377.00	3,369	540.842	0.15815	0.08603			0.03
	376.03	**6,949**	**551.35**		**0.08907**	**6.176**	**2,616**	
P10_10A2	376.45	6,949	550.879	0.07033	0.08852			0.025
P10_10A3	377.08	6,949	550.175	0.15813	0.08779			0.025
	375.82	**13,3737**	**565.28**		**0.09285**	**6.634**	**2,476**	
P10_20A2	375.99	13,373	565.118	0.07027	0.09290			0.025
P10_20B2	376.28	13,373	564.834	0.10969	0.09291			0.026
P10_20A3	376.65	13,373	564.473	0.15789	0.09270			0.026
P10_20B3	377.22	13,373	563.915	0.21482	0.09239			0.027
P10_20A4	377.68	13,373	563.465	0.28015	0.09265			0.025
P10_20B4	378.14	13,373	563.014	0.35441	0.09257			0.025
ý**376.02**	**20,437**	**577.41**		**0.09785**	**6.603**	**2,566**		
P10_30A2	376.53	20,437	576.960	0.07039	0.09762			0.028
P10_30B2	376.64	20,437	576.863	0.1099	0.09778			0.026
P10_30A3	377.01	20,437	576.538	0.15824	0.09766			0.017
O10_30B3	377.18	20,437	576.388	0.21500	0.09787			0.025
P10_30A4	377.68	20,437	575.948	0.28064	0.09739			0.025
	375.82	**27,374**	**587.83**		**0.1010**	**6.808**	**2.524**	
P10_40A2	376.12	27,374	587.591	0.07025	0.1011			0.025
P10_40B2	376.60	27,374	587.202	0.10978	0.1010			0.017
P10_40A3	376.57	27,374	587.227	0.15788	0.1012			0.025
P10_40B3	376.98	27,374	586.894	0.21478	0.1013			0.025
P10_40A4	377.39	27,374	586.562	0.28005	0.1012			0.025
P10_40B4	377.88	27,374	586.165	0.35396	0.1013			0.017
	375.97	**34,170**	**596.53**		**0.1048**	**6.975**	**2,519**	
P10_50A3	376.88	34,170	595.836	0.15803	0.1049			0.025
P10_50B3	376.86	34,170	595.851	0.15802	0.1047			0.025
P10_50C3	377.22	34,170	595.578	0.21478	0.1049			0.025
P10_50D3	377.23	34,170	595.570	0.21500	0.1048			0.025
P10_50A4	377.60	34,170	595.289	0.28036	0.1048			0.025
P10_50B4	377.59	34,170	595.297	0.28029	0.1049			0.025
P10_50C4	377.93	34,170	595.039	0.35441	0.1048			0.025
P10_50D4	377.92	34,170	595.047	0.35452	0.1048			0.025
	401.43	**3,356**	**508.26**		**0.08049**	**5.287**	**2,995**	
P12_05A2	402.00	3,356	507.439	0.06420	0.08021			0.055
P12_05B2	402.17	3,356	507.192	0.10023	0.08052			0.045
P12_05A3	402.41	3,356	506.843	0.14423	0.08007			0.05
	401.39	**6,762**	**521.00**		**0.08308**	**5.545**	**2,876**	
P12_10A2	401.77	6,762	520.529	0.06325	0.08318			0.05
P12_10B2	401.94	6,762	520.317	0.09880	0.08270			0.045
P12_10A3	402.16	6,762	520.042	0.14223	0.08309			0.04
	401.53	**13,590**		**0.08961**	**5.860**	**2,832**		
P12_20A2	402.17	13,590	539.327	0.06332	0.08847			0.05

Table II. *(Continued)*

ID No.	T (K)	P (kPa)	ρ ($kg \cdot m^{-3}$)	q ($W \cdot m^{-1}$)	λ ($W \cdot m^{-1} \cdot K^{-1}$)	α ($10^{-8} m^2 \cdot s^{-1}$)	C_p ($J \cdot kg^{-1} \cdot K^{-1}$)	B (s^{-1})
P12_20B2	402.22	13,590	539.275	0.09886	0.08905			0.06
P12_20A3	402.35	13,590	539.141	0.14226	0.08834			0.055
P12_20B3	402.59	13,590	538.893	0.19358	0.08817			0.056
	401.32	**20,505**	**554.97**		**0.09377**	**6.242**	**2,707**	
P12_30A2	401.72	20,505	554.610	0.06331	0.09360			0.058
P12_30B2	401.90	20,505	554.447	0.09885	0.09365			0.035
P12_30A3	402.11	20,505	554.256	0.14222	0.09309			0.035
P12_30B3	402.35	20,505	554.039	0.19343	0.09384			0.035
	401.44	**27,304**	**566.81**		**0.09638**	**6.585**	**2,582**	
P12_40A2	401.80	27,304	566.509	0.06326	0.09657			0.03
P12_40B2	402.02	27,304	566.327	0.09883	0.09720			0.035
P12_40A3	402.23	27,304	566.154	0.14221	0.09703			0.035
P12_40B3	402.49	27,304	565.940	0.19339	0.09736			0.04
	401.41	**34,261**	**577.29**		**0.1013**	**6.805**	**2,579**	
P12_50A2	401.78	34,261	577.007	0.06327	0.1012			0.05
P12_50B2	401.95	34,261	576.878	0.09881	0.1010			0.05
P12_50A3	402.14	34,261	576.733	0.14221	0.1008			0.05
	428.12	**3,634**	**466.67**		**0.07676**	**5.114**	**3,216**	
P15_05A2	428.58	3,634	465.820	0.06840	0.07736			0.055
P15_05B2	428.59	3,634	465.802	0.06839	0.07760			0.058
P15_05C2	428.85	3,634	465.322	0.10698	0.07788			0.055
	428.21	**6,560**	**484.05**		**0.08031**	**5.354**	**3,099**	
P15_10A2	428.66	6,560	483.390	0.06844	0.08010			0.05
P15_10B2	428.68	6,560	483.361	0.06848	0.08036			0.055
P15_10C2	428.88	6,560	483.067	0.10701	0.08084			0.06
	428.19	**13,635**	**511.74**		**0.08557**	**5.678**	**2,945**	
P15_20A2	428.66	13,635	511.226	0.06844	0.08514			0.05
P15_20B2	428.66	13,635	511.226	0.06848	0.08478			0.045
P15_20C2	428.87	13,635	510.994	0.10695	0.08438			0.035
P15_20D2	428.88	13,635	510.983	0.10695	0.08403			0.05
	428.23	**20.489**	**530.15**		**0.09067**	**6.032**	**2,835**	
P15_30A2	428.71	20,489	529.699	0.06846	0.09002			0.05
P15_30B2	428.88	20,489	529.540	0.10699	0.08981			0.04
P15_30A3	429.14	20,489	529.296	0.15396	0.08933			0.04
	428.29	**27,239**	**544.37**		**0.09284**	**6.131**	**2,782**	
P15_40A2	428.76	27,239	543.975	0.06848	0.09272			0.05
P15_40B2	429.01	27,239	543.765	0.10698	0.09281			0.06
P15_40A3	429.29	27,239	543.530	0.15398	0.09265			0.044
	428.26	**24,357**	**556.90**		**0.09756**	**6.365**	**2,752**	
P15_50A2	428.74	34,357	556.529	0.06845	0.09704			0.05
P15_50B2	428.93	34,357	556.384	0.10694	0.09649			0.055
P15_50A3	429.18	34,357	556.192	0.15391	0.09640			0.052

First, one must be able to distinguish between the onset of free convection and the influence of fluid radiation. This can be illustrated by comparing a measurement in a nonradiation participating fluid, such as argon, with one made in *n*-pentane. The commencement of free convection can be detected by a departure from the straight line formed of the corrected temperature difference, $\Delta T \sim \ln(t)$, data provided that one is remote from regions where outer boundary effects can be observed [5]. In Fig. 2 a measurement of corrected temperature difference over a 2-s period made on argon at 323.56 K and 20.93 MPa [$\lambda_0 = 0.02852\ \mathrm{W \cdot m^{-1} \cdot K^{-1}}$, $\alpha_0 = 12.35 \times 10^{-8}\ \mathrm{m^2 \cdot s}$ (ID No. A50_30A3 [11])] is shown. The deviation from a linear fit of the corrected temperature difference with t is indicated in Fig. 3, where after 1.7 s the departure from linearity indicates the onset of convection. Table III indicates that as the time frame for the determination of λ from the data set is extended and/or contracted from 0.12 to 1 and then 1.7 s, there is no significant ($\leqslant 0.2\%$) difference in the value of λ returned. The modified Raleigh number, $\mathrm{Ra} = g\beta \Delta T \delta^3/(\nu\alpha)$, for the commencement of convection for this measurement is 1.3×10^5, a value that compares favorably with the predicted "critica" criterion $\mathrm{Ra} \geqslant 10^5$ based upon the conduction layer thickness at time t [16].

The exact determination of the influence of fluid thermal radiation requires consideration of the full form of the appropriate integral-differential energy equation. Its numerical solution was obtained, for a range of

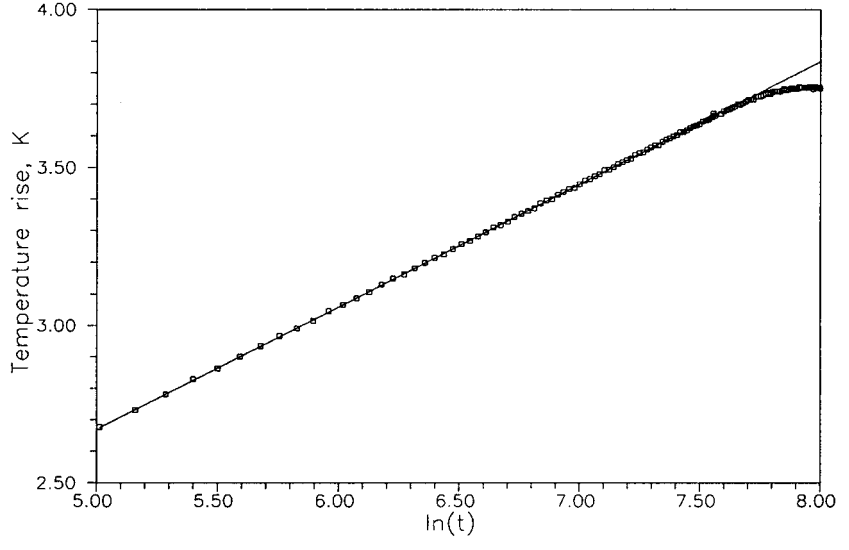

Fig. 2. Temperature rise as a function of $\ln(t)$ for a measurement on argon at 323 K and 20.9 MPa (run ID No. A50_30A3 [11]).

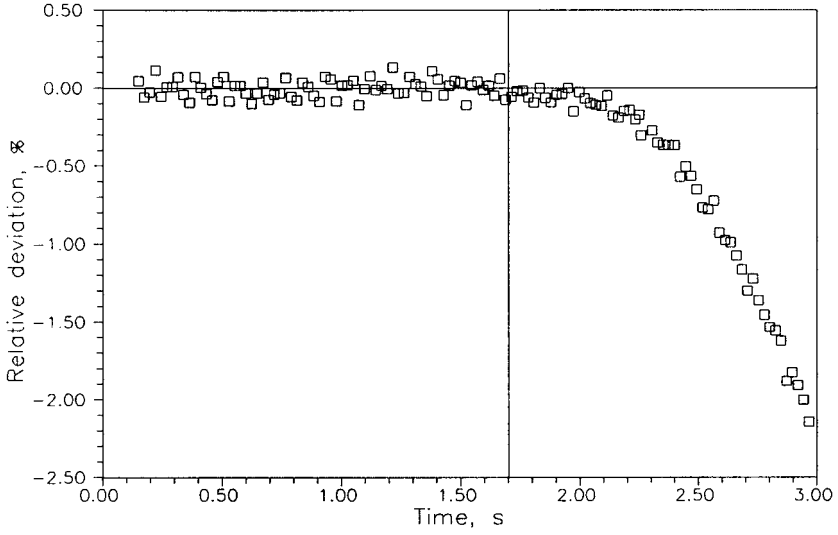

Fig. 3. Deviation of the temperature rise from the linear fit versus $\ln(t)$ for a measurement on argon at 323 K and 20.9 MPa (run ID No A50_30A3 [11]).

applicable instrument conditions and selected fluids in the *n*-alkane series, by Ref. 9. Here the deviation of the temperature rise of the hot wire was simulated for measurements in *n*-heptane from the best-fit straight line. Figure 6 in Ref. 9 clearly indicates the curvature that may be expected in these fluids. This figure should be compared to Fig. 4, where comparable measurements are shown for a variety of wire powers for *n*-pentane. In this example, the corrected (aside from fluid radiation emission) $\Delta T \sim \ln(t)$ data indicate, from the start, a consistent departure from linearity *for all times* with a shape that corresponds, almost exactly, to that indicated in Ref. 9. In Ref. 17, however, these same authors stated for *n*-heptane "that the effects of radiation introduce no significant curvature to the experimental

Table III. Thermal Conductivity of Argon at 323.56 K and 20.93 MPa with $q = 0.13915\ \mathrm{W \cdot m^{-1}}$ ($\lambda_0 = 0.02852\ \mathrm{W \cdot m^{-1} \cdot K^{-1}}$, $\chi = 0.0007302\ \mathrm{K^{-1}}$ (ID No. A50_30A3 [11])

Time frame (s)	λ ($\mathrm{W \cdot m^{-1} \cdot K^{-1}}$)	T_r (K)
0.12–1.00	0.02857	326.53
0.12–1.70	0.02852	326.63
1.00–1.70	0.02852	327.07

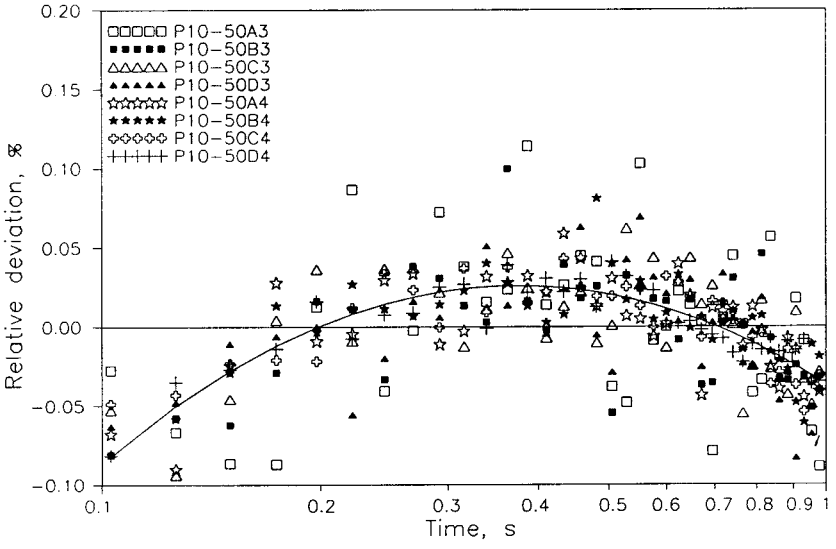

Fig. 4. Deviations of the corrected (aside from fluid radiation) temperature differences from the best-fit straight line for a series of *n*-pentane experiments near 376 K and 34.2 MPa.

line." Table IV illustrates that as the correction for fluid radiation to the *n*-pentane data of Fig. 4 is implemented, the goodness of fit, as expressed by the data's standard deviation, improves substantially, and thus indicates that the present corrected measurements, especially at higher power levels, may have a reproducibility of better than $\pm 0.02\%$.

Table IV. Standard Deviation of the Corrected Temperature Rise from the Best-Fit Straight Line Before and After Correction for Fluid Radiation for a Series of Experimental Runs Near 376 K and 34.2 MPa

		SD (%)	
Run ID (Table II)	Power ($W \cdot m^{-1}$)	Before corr.	After corr.
P10_50A3	0.15803	0.050	0.043
P10_50B3	0.15802	0.034	0.030
P10_50C3	0.21478	0.033	0.024
P10_50D3	0.21500	0.032	0.025
P10_50A4	0.28036	0.032	0.019
P10_50B4	0.28029	0.027	0.014
P10_50C4	0.35441	0.029	0.012
P10_50D4	0.35452	0.025	0.011

The full correction method proposed in Ref. 9 was time-consuming and computationally intensive and could not be directly applied to the experimental procedure. Nieto de Castro [7] showed that an approximate correction procedure could be implemented to account for the fluid radiation emission characteristics, although, as indicated earlier, the inner boundary condition was inappropriate. The revision of their analysis results in a correction only slightly different as illustrated in Figs. 5 and.6, where the uncorrected and fluid radiation-corrected temperature differences are shown as functions of time for an *n*-pentane measurement. In this example, the value of fluid radiation correction B necessary to restore linearity is 0.025 s^{-1}—an empirical value determined through the use of Eq. (3). The values of B used are tabulated in Table II and shown in Fig. 7. It can be seen that there is a systematic decrease in B with an increase in density and that its value increases with temperature, though with a greater spread. It should be noted that for the measurement above, Ra is only 8330 and there is no convection despite the extension of the time measurement to 2 s.

For accurate thermal diffusivity results, the measured values must first be corrected for the temperature variation in properties over time [Eq. (8)]. Figure 8 illustrates the variation in thermal diffusivity values determined as a function of power after this correction for the series of data points

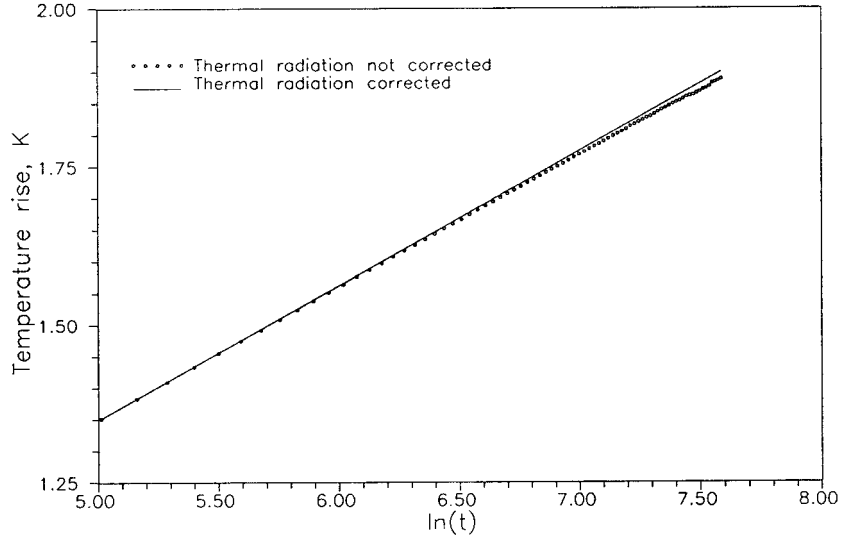

Fig. 5. $\Delta T \sim \ln(t)$ before and after fluid thermal radiation corrections: normal pentane at 376 K and 34.17 MPa and a power of 0.28036 $W \cdot m^{-1}$ (run ID No. P10_50A4).

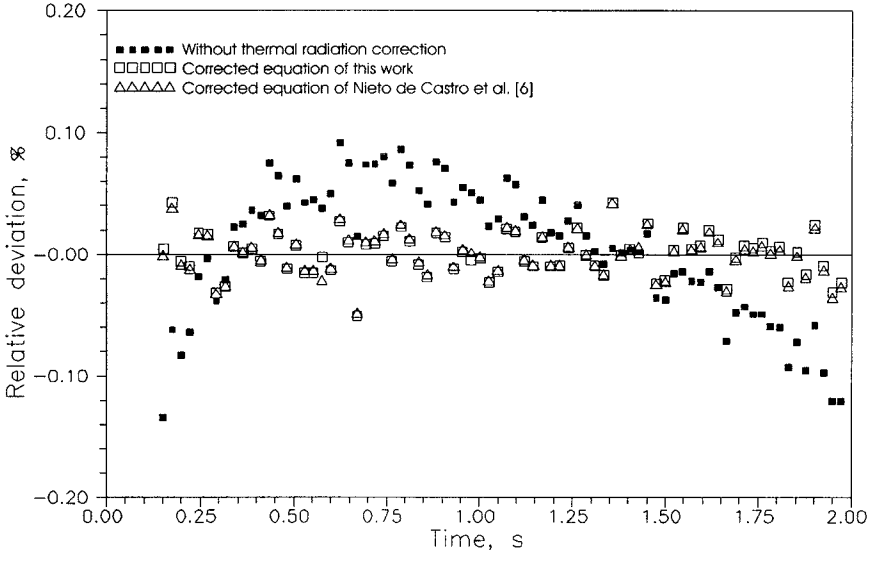

Fig. 6. Deviation of uncorrected and fluid radiation-corrected temperature rise from the linear fit: normal pentane at 376 K and 34.17 MPa and a power of 0.28036 $W \cdot m^{-1}$ (run ID No. P10_50A4).

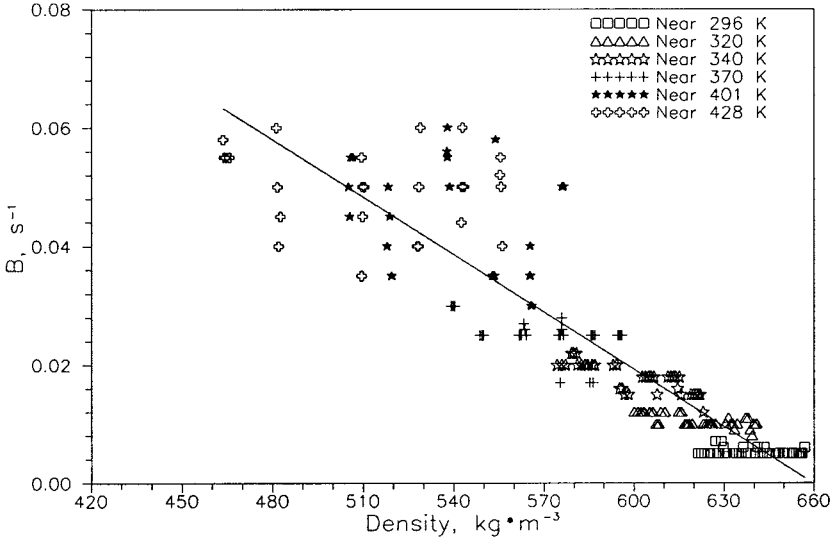

Fig. 7. Value of B as a function of density for *n*-pentane.

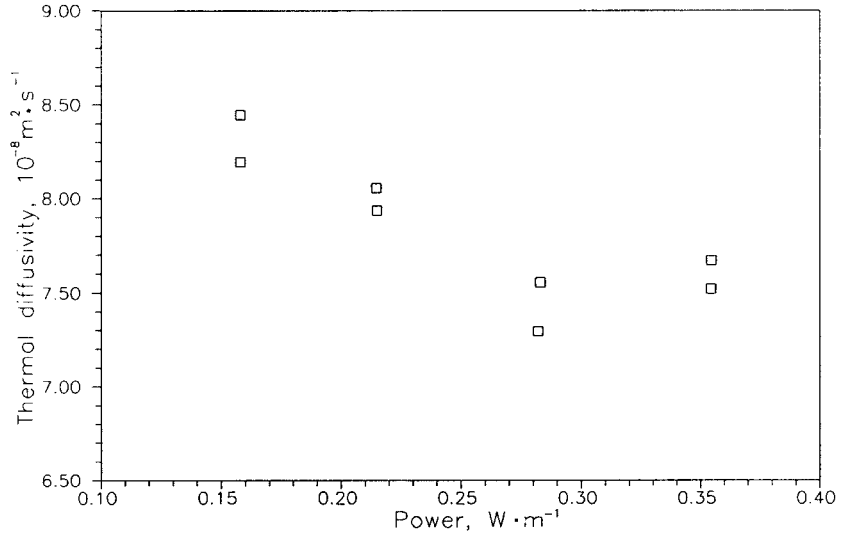

Fig. 8. Thermal diffusivity on *n*-pentane at different powers before correcting the temperature offset due to bridge imbalance.

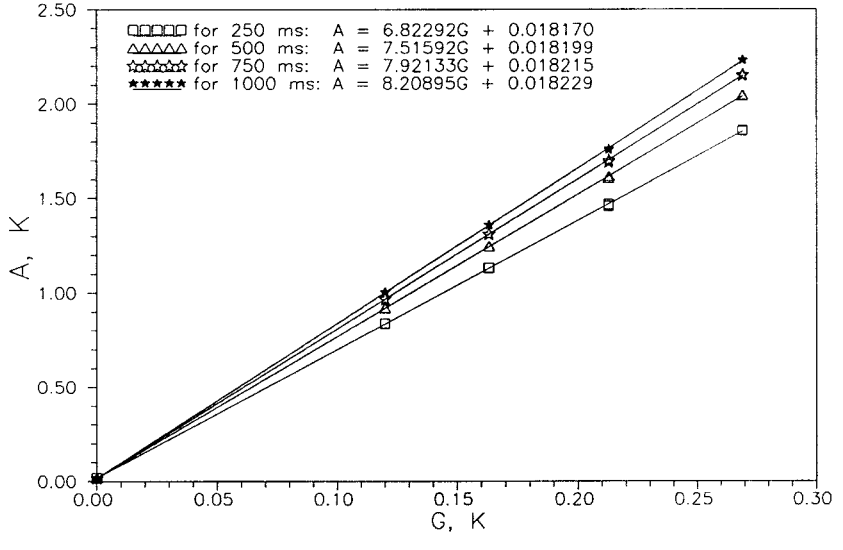

Fig. 9. Temperature rise of the hot wire at different powers and times.

(ID Nos. P10_50A3 to P10_50D4); a clear dependency on power is seen despite very careful attention to bridge balance. To clarify this dependency, Table V shows the temperature rise of the hot wire, denoted A, as a function of $G = q/(4\pi\lambda_0)$, the gradient, with values determined at selected times. The temperature rise at identical times, but for different energy inputs, can be seen fit to straight lines as a function of power. According to Eq. (8), if the square term in G is ignored, the vertical intercepts of these lines should be zero; however, as indicated in Fig. 9, the intercept clearly shows a constant value of 18.2 ± 0.03 mK. It thus appears that, despite the careful bridge balance, there is a systematic and reproducible "offset" in the temperature rise that can be considered as a "zero"-time bridge or system temperature difference.

From Eq. (1),

$$\alpha = \frac{a^2 C}{4t} e^{A/G} \tag{9}$$

and thus an error introduced to the thermal diffusivity due to an error in A is

$$\frac{\delta\alpha}{\alpha} = \frac{\delta A}{G} \tag{10}$$

Therefore, although uncertainty in A may be small, apparent errors of between 1 and 15% in thermal diffusivity can be introduced (G in Table V). The determination of this correction is therefore essential to obtain accurate and reproducible thermal diffusivity values. Figure 10 shows the deviations of the eight individually measured thermal diffusivity at the

Table V. Temperature Rise of the Hot-Wire as a Function of G (ID Nos. P10_50A3 to P10_50D4)

	A (K)			
G (K)	At 0.25 s	At 0.5 s	At 0.75 s	At 1.0 s
0.11992	0.83663	0.91975	0.96838	1.00288
0.11993	0.83880	0.92189	0.97049	1.00498
0.16300	1.13276	1.24573	1.31182	1.35871
0.16317	1.13257	1.24574	1.31194	1.35891
0.21271	1.45809	1.60558	1.69186	1.75308
0.21277	1.46765	1.61517	1.70146	1.76268
0.26897	1.85460	2.04101	2.15006	2.22743
0.26905	1.86005	2.04648	2.15554	2.23292

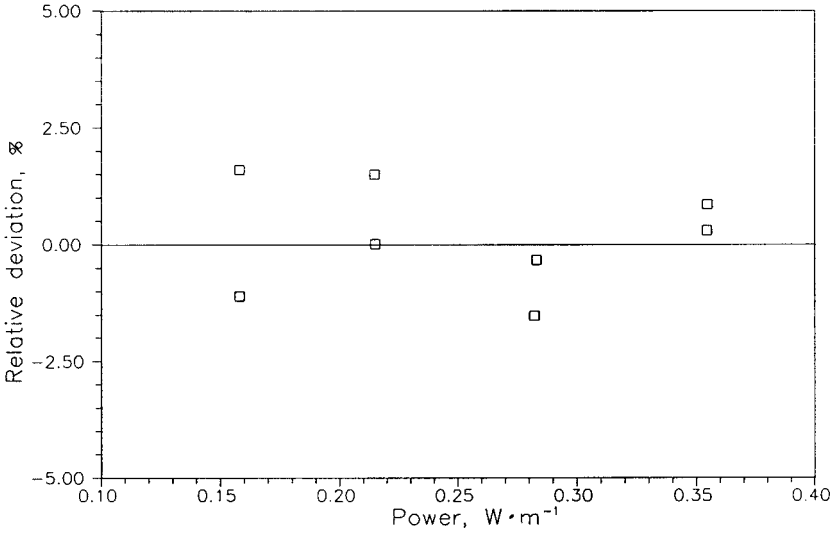

Fig. 10. Deviation in the corrected thermal diffusivity from that obtained via the gradient of the linear regression of $\Delta T \sim G$ after correcting for the influence of temperature offset.

equilibrium thermostat temperature before and after correcting for the influence of temperature offset from the value obtained via the gradient of linear regression of $\Delta T \sim q/(4\pi\lambda)$, which is indicated in boldface in Table II along with the corresponding thermal conductivity and isobaric specific heat determinations.

Once corrected, all the thermal conductivity and thermal diffusivity values were correlated with expressions of the form

$$\lambda(T, \rho) = \lambda_0(T) + \Delta\lambda(\rho) = \lambda_0(T) + a_0(1 + a_1\rho + a_2\rho^2) \tag{11}$$

and

$$\alpha \times 10^8 = b_0[1 + b_1\rho + b_2\rho^2] \tag{12}$$

where $\Delta\lambda$ is the excess thermal conductivity and λ_0 is the ideal-gas, or zero-density, value, which is a unique function of temperature. The coefficients for these equations are listed in Table VI. The value of λ_0 was obtained by fitting the thermal conductivity data for *n*-pentane vapor at zero density [15],

$$\lambda_0 = 1.2725 \times 10^{-7}T^2 + 1.43929 \times 10^{-5}T - 0.00156006 \tag{13}$$

Table VI. Correlation Coefficients for Excess Thermal Conductivity and Thermal Diffusivity of *n*-Pentane

Excess thermal conductivity	Thermal diffusivity
$a_0 = 0.301551$	$b_0 = 16.7307$
$a_1 = -1.163789 \times 10^{-3}$	$b_1 = -5.56875 \times 10^{-2}$
$a_2 = 1.33933 \times 10^{-6}$	$b_2 = 6.61475 \times 10^{-5}$

In Eqs. (11)–(13) λ, λ_0, and $\Delta\lambda$ are in units of $W \cdot m^{-1} \cdot K^{-1}$, temperature is in K, ρ is in $kg \cdot m^{-3}$, and α is in $m^2 \cdot s^{-1}$. Figures 11 and 12 show the thermal conductivity and thermal diffusivity values as functions of density. Figures 13 and 14 indicate the experimental deviations in the thermal conductivity and thermal diffusivity from the corresponding correlations and the available data. From Fig. 12, it can be seen that the maximum deviation of the thermal conductivity from that given by Eq. (11) is less than 2%.

The measurements obtained by Carmichael et al. [2] were obtained using a steady-state spherical shell instrument of about 89-mm diameter with temperature differences of between 1 and 3 K across a 0.508-mm gap —these data are systematically lower than Eq. (11) by between 4 and 5%.

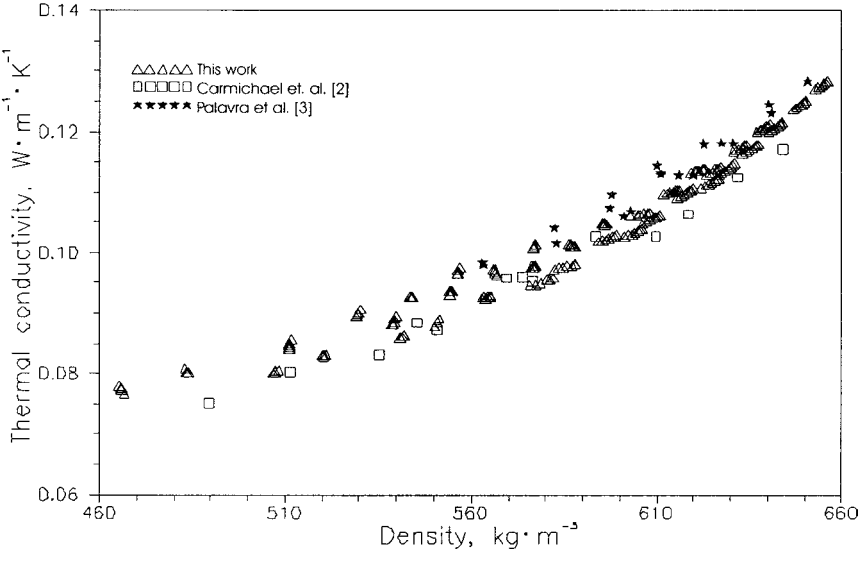

Fig. 11. Thermal conductivity of *n*-pentane as a function of density.

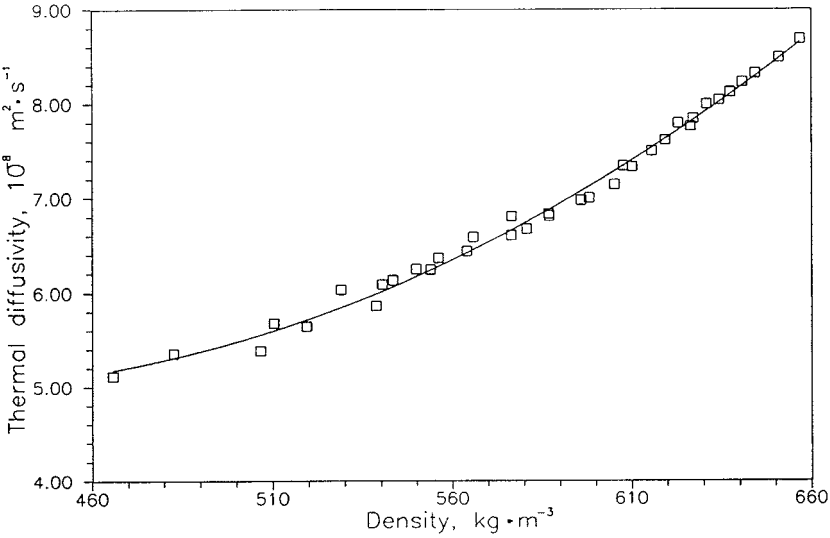

Fig. 12. Thermal diffusivity of *n*-pentane as a function of density.

The data of Palavra et al. [3] were obtained using a transient hot-wire instrument with a claimed uncertainty of $\pm 0.5\%$; it was unclear if any radiation corrections were made to the data since, although referring to Ref. 16, no details of the uncorrected data were given. The deviations of this set of measurements from Eq. (11) increase systematically with temperature to a maximum value of $+8\%$; however, as the density increases, the measurements fall to within $+2\%$.

From Fig. 14 it can be seen that the standard deviation of the thermal diffusivity data represented by Eq. (12) is less than $\pm 2\%$. This correlation and its data appear to be the only ones available for this fluid.

Derived isobaric specific heats, determined using the equation of state [14], are shown as a function of density in Fig. 15. The deviations of these results from specific heat values given by Ref. 14 are indicated in Fig. 16, and it can be seen that only at low densities do the present data depart by about $+4\%$, while in the higher-density range the maximum deviations do not exceed $\pm 2\%$.

5. CONCLUSION

The thermal conductivity and thermal diffusivity of liquid *n*-pentane have been measured using a new transient hot-wire instrument over the temperature range of 293 to 428 K at pressures from 3.5 to 35 MPa. The

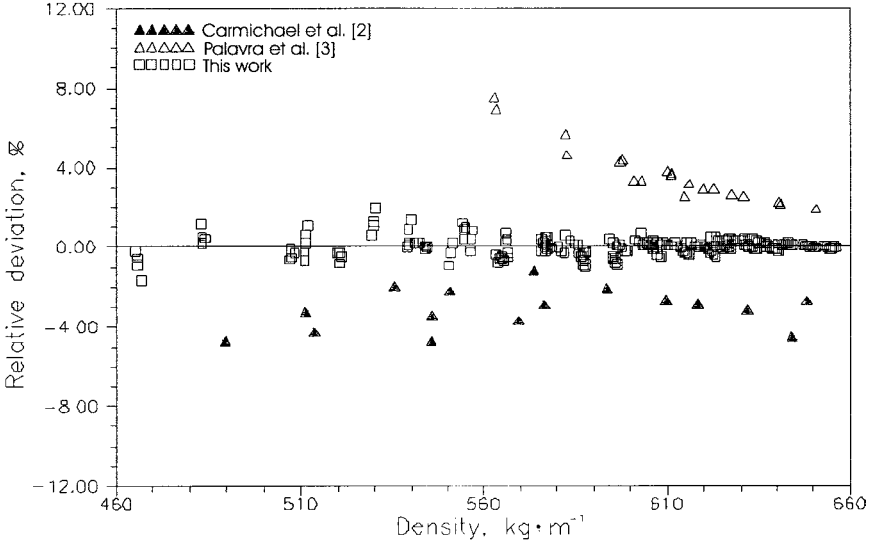

Fig. 13. Deviations in the thermal conductivity from different sources from Eq. (11).

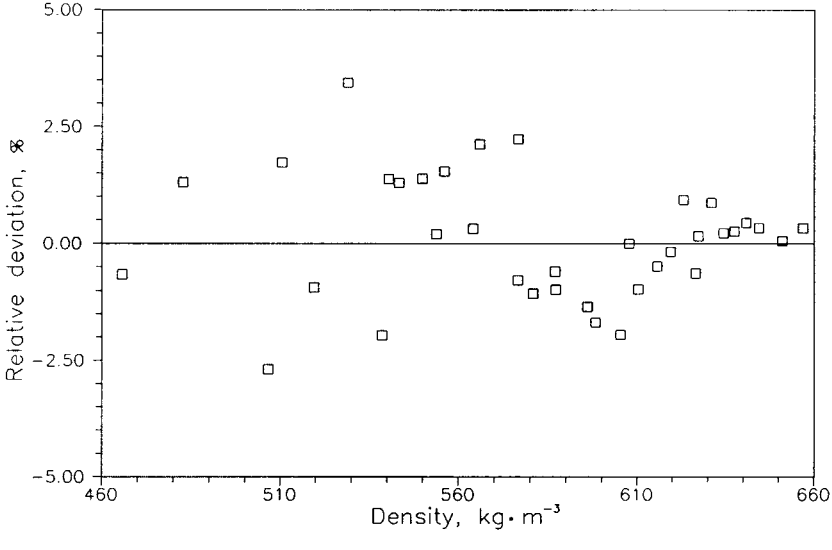

Fig. 14. Deviations in the thermal diffusivity from Eq. (12).

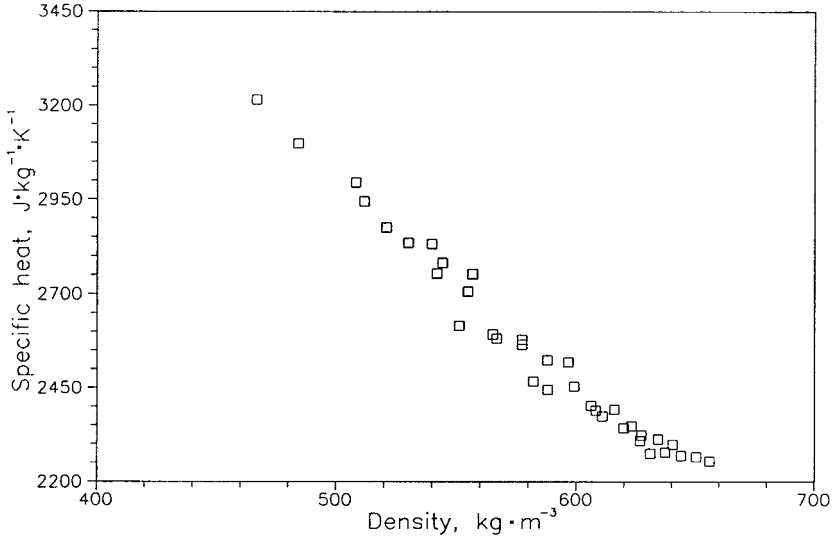

Fig. 15. Derived isobaric specific heat of *n*-pentane as a function of density.

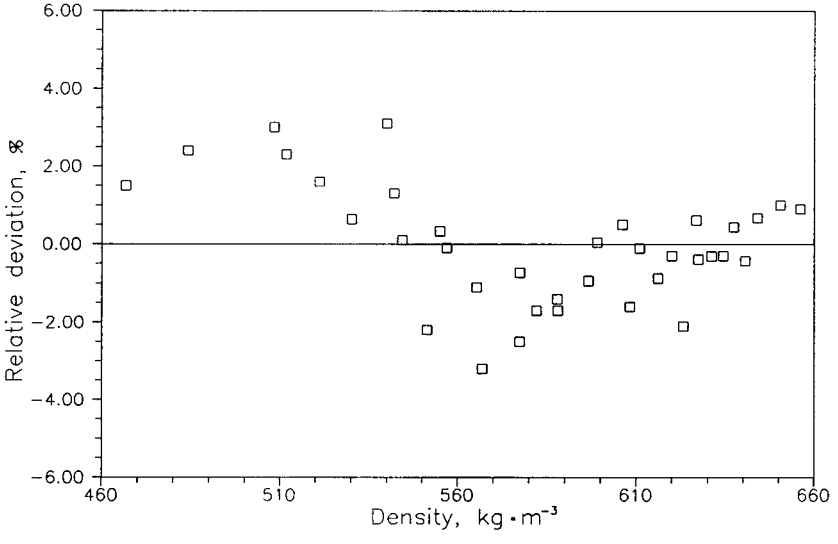

Fig. 16. Deviation of the derived isobaric specific heat from that obtained from the *NIST*12 Database [15].

measured data, corrected for fluid thermal radiation, are estimated to have an uncertainty of $\pm 5\%$ for thermal conductivity and $\pm 2\%$ for thermal diffusivity. The excess thermal conductivity and thermal diffusivity were correlated as functions of density. The uncertainty in the correlations is estimated to be less than $\pm 2\%$.

APPENDIX. INFLUENCE OF FLUID RADIATION

The model for thermal radiation can be described by the following equations: at $t > 0$ and $0 \leqslant r \leqslant a$,

$$\frac{\partial^2 \Delta T_1}{\partial r^2} + \frac{1}{r}\frac{\partial \Delta T_1}{\partial r} - \frac{1}{\alpha_1}\frac{\partial \Delta T_1}{\partial t} = -\frac{q}{\pi a^2 \lambda_1} \tag{A.1}$$

at $t > 0$ and $r > a$,

$$\frac{\partial^2 \Delta T_2}{\partial r^2} + \frac{1}{r}\frac{\partial \Delta T_2}{\partial r} - \frac{1}{\alpha_2}\frac{\partial \Delta T_2}{\partial t} = f\,\Delta T_2 \tag{A.2}$$

where

$$f = \frac{16 K n^2 \sigma T_0^3}{\lambda_2} \tag{A.3}$$

and the boundary and initial conditions are

$$r = 0, \qquad \frac{\partial \Delta T_1}{\partial r} = 0 \tag{A.4}$$

$$r = a, \qquad \Delta T_1 = \Delta T_2, \qquad \lambda_1 \frac{\partial \Delta T_1}{\partial r} = \lambda_2 \frac{\partial \Delta T_2}{\partial r} \tag{A.5}$$

$$r \to \infty, \qquad \Delta T_2 = 0 \tag{A.6}$$

$$t \leqslant 0, \qquad 0 \leqslant r < \infty, \qquad \Delta T_1 = \Delta T_2 = 0 \tag{A.7}$$

Here λ and α represent the thermal conductivity and thermal diffusivity, respectively; the subscripts 1 and 2 represent the wire and the fluid, respectively, σ is the Stephan–Boltzmann coefficient, K is the mean absorption coefficient, and n is the refractive index of the fluid. After Laplace

transformation, the differential equations, as well as the boundary and initial conditions, are

$$\frac{\partial^2 \Delta\bar{T}_1}{\partial r^2}+\frac{1}{r}\frac{\partial \Delta\bar{T}_1}{\partial r}-\frac{p}{\alpha_1}\Delta\bar{T}_1=-\frac{q}{p\pi a^2\lambda_1} \tag{A.8}$$

$$\frac{\partial^2 \Delta\bar{T}_2}{\partial r^2}+\frac{1}{r}\frac{\partial \Delta\bar{T}_2}{\partial r}-\left(\frac{p}{\alpha_2}+f\right)\Delta\bar{T}_2=0 \tag{A.9}$$

$$r=0, \qquad \frac{\partial \Delta\bar{T}_1}{\partial r}=0 \tag{A.10}$$

$$r=a, \qquad \lambda_1\left(\frac{\partial \Delta\bar{T}_1}{\partial r}\right)=\lambda_2\left(\frac{\partial \Delta\bar{T}_2}{\partial r}\right), \qquad \Delta T_1=\Delta T_2 \tag{A.11}$$

$$r\to , \qquad \Delta T_2=0 \tag{A.12}$$

Let $q_1=\sqrt{p/\alpha_1}$, $q_2=\sqrt{p/\alpha_2+f}$, $x_1=q_1 r$, $x_2=q_2 r$; then Eqs. (A.8) and (A.9) can be rewritten

$$\frac{\partial^2 \Delta\bar{T}_1}{\partial x_1^2}+\frac{1}{x_1}\frac{\partial \Delta\bar{T}_1}{\partial x_1}-\Delta\bar{T}_1=-\frac{q\alpha_1}{p^2\pi a^2\lambda_1} \tag{A.13}$$

$$\frac{\partial^2 \Delta\bar{T}_2}{\partial x_2^2}+\frac{1}{x_2}\frac{\partial \Delta\bar{T}_2}{\partial x_2}-\Delta\bar{T}_2=0 \tag{A.14}$$

with the solution

$$\Delta\bar{T}_1=G\left[\frac{q_2\lambda_2 K_1(q_2a)\,I_0(q_1a)}{q_1\lambda_1 I_1(q_1a)\,K_0(q_2a)+q_2\lambda_2 K_1(q_2a)\,I_0(q_1a)}-1\right] \tag{A.15}$$

where $G=-(q\alpha_1)/(p^2\pi a^2\lambda_1)$ or, using the approximate forms of the Bessel functions, the solution has the form

$$\Delta\bar{T}_1=GB/A \tag{A.16}$$

where

$$B=1+\tfrac{1}{4}q_1^2r^2+\tfrac{1}{2}q_2^2a^2\ln(\tfrac{1}{2}Cq_2a)+\tfrac{1}{8}q_1^2q_2^2a^2r^2\ln(\tfrac{1}{2}Cq_2a)-\tfrac{1}{4}q_2^2a^2-\tfrac{1}{16}q_1^2q_2^2a^2r^2 \tag{A.17}$$

and

$$A = 1 + \frac{1}{2} q_2^2 a^2 \ln\left(\frac{1}{2} C q_2 a\right) - \frac{1}{4} q_2^2 a^2 + \frac{1}{4} q_1^2 a^2 + \frac{1}{8} q_1^2 q_2^2 a^4 \ln\left(\frac{1}{2} C q_2 a\right) - \frac{1}{16} q_1^2 q_2^2 a^4 - \frac{\lambda_1}{2\lambda_2} q_1^2 a^2 \ln\left(\frac{1}{2} C q_2 a\right) - \frac{\lambda_1}{8\lambda_2} q_1^2 q_2^2 a^4 \ln\left(\frac{1}{2} C q_2 a\right) + \frac{\lambda_1}{8\lambda_2} q_1^2 q_2^2 a^4 \tag{A.18}$$

Multiply the numerator and the denominator by $(-A+2)$ and ignore terms which contain a^4 or higher order and consider the denominator to be approximately 1. A polynomial approximate solution for $\Delta\bar{T}_1$ results.

$$\Delta\bar{T}_1 = G\left[\frac{1}{4} q_1^2 r^2 - \frac{1}{4} q_1^2 a^2 + \frac{\lambda_1}{2\lambda_2} q_1^2 a^2 \ln\left(\frac{1}{2} C q_2 a\right) + \frac{\lambda_1}{4\lambda_2} q_1^2 q_2^2 a^4 \ln\left(\frac{1}{2} C q_2 a\right) - \frac{\lambda_1}{8\lambda_2} q_1^2 q_2^2 q^4 - \frac{\lambda_1}{4\lambda_2} q_1^2 q_2^2 a^4 \ln^2\left(\frac{1}{2} C q_2 a\right) - \frac{1}{16} q_1^4 q^2 r^2 + \frac{1}{16} q_1^4 a^4 - \frac{\lambda_1}{4\lambda_2} q_1^4 a^4 \ln\left(\frac{1}{2} C q_2 a\right) + \frac{\lambda_1}{8\lambda_2} q_1^4 a^2 r^2 + \frac{\lambda_1^2}{4\lambda_2^2} q_1^4 a^4 \ln^2\left(\frac{1}{2} C q_2 a\right)\right] \tag{A.19}$$

if $f = 0$, the inverse Laplace transformation of Eq. (A.19), i.e., the solution for ΔT_1 can be written [4]

$$\Delta T_1' = \frac{q}{4\pi\lambda_2}\left[1 - \frac{a^2}{2\lambda_2 t}\left(\frac{\lambda_1}{\alpha_1} - \frac{\lambda_2}{\alpha_2}\right)\right] \ln\frac{4\alpha_2 t}{a^2 C} + \frac{q}{4\pi\lambda_2}\left[\frac{\lambda_2}{\lambda_1}\left(1 - \frac{r^2}{a^2}\right) + \frac{a^2}{2\alpha_2 t} - \frac{a^2}{2\alpha_1 t} + \frac{r^2}{4\alpha_1 t}\right] \tag{A.20}$$

which is the approximate solution for the case when the effect of fluid thermal radiation is not present.

If $f \neq 0$, the approximation

$$\ln q_2 = \ln\left(\sqrt{\frac{p}{\alpha_2}}\right) + \frac{1}{2}\left(\frac{f\alpha_2}{p} - \frac{f^2\alpha_2^2}{p^2}\right) \tag{A.21}$$

allows the inverse Laplace transformation, ignoring all the terms containing f^2 or higher, and the approximate solution

$$\Delta T_1 = \Delta T_1' + \frac{f a^2 q \lambda_1 \alpha_2}{8\pi\lambda_2^2 \alpha_1} \ln \frac{4\alpha_2 t}{a^2 C} + \frac{qf(r^2 - a^2)}{16\pi\lambda_2} \ln \frac{4\alpha_2 t}{a^2 C}$$

$$+ \frac{qfa^2}{16\pi\lambda_2} \left(\ln^2 \frac{4\alpha_2 t}{a^2 C} - \frac{\pi^2}{6} \right) - \frac{qf\alpha_2 t}{4\pi\lambda_2} - \frac{qfa^2}{8\pi\lambda_2} \tag{A.22}$$

If the effects of the thermophysical properties of the hot wire are not considered, but the wire is considered finite, the model can be described by

$$\frac{\partial^2 \Delta T_2}{\partial r^2} + \frac{1}{r} \frac{\partial \Delta T_2}{\partial r} - \frac{1}{\alpha_2} \frac{\partial \Delta T_2}{\partial t} = f \Delta T_2 \tag{A.23}$$

$$r = a, \qquad \frac{\partial \Delta T_2}{\partial r} = -\frac{q}{2\pi\lambda_2 a} \tag{A.24}$$

$$r \to \infty, \qquad \Delta T_2 = 0 \tag{A.25}$$

$$t \leqslant 0, \qquad \Delta T_2 = 0 \tag{A.26}$$

After Laplace transformation the equations are

$$\frac{\partial^2 \Delta \bar{T}_2}{\partial r^2} + \frac{1}{r} \frac{\partial \Delta \bar{T}_2}{\partial r} - \frac{p}{\alpha_2} \Delta \bar{T}_2 = f \Delta \bar{T}_2 \tag{A.27}$$

$$r = a, \qquad \frac{\partial \Delta \bar{T}_2}{\partial r} = -\frac{q}{2\pi\lambda_2 a p} \tag{A.28}$$

$$r \to \infty, \qquad \Delta \bar{T}_2 = 0 \tag{A.29}$$

and of $q_2 = \sqrt{p/\alpha_2 + f}$, the solution can be obtained as

$$\Delta \bar{T}_2 = c_1 I_0(q_2 r) + c_2 K_0(q, r) \tag{A.30}$$

According to the boundary condition at $r \to \infty$, $c_1 = 0$. Using the boundary condition at $r = a$.

$$c_2 = \frac{G}{q_2 K_1(q_2 a)} \tag{A.31}$$

where

$$G = -\frac{q}{2\pi\lambda_2 ap} \tag{A.32}$$

$$\Delta\bar{T}_2 = -\frac{GK_0(q_2 r)}{q_2 K_1(q_2 a)} \tag{A.33}$$

Using the previous methods, the approximate solution for $\Delta\bar{T}_2$ at $r = a$ can be obtained as

$$\Delta\bar{T}_2 = G[a\ln(\tfrac{1}{2}Cq_2a) + \tfrac{1}{2}q_2^2a^3\ln(\tfrac{1}{2}Cq_2a) - \tfrac{1}{4}q_2^2a^3 - \tfrac{1}{2}q_2^2a^3\ln^2(\tfrac{1}{2}Cq_2a) \tag{A.34}$$

Considering $\ln q_2 \approx \ln\sqrt{p/k_2} + fk_2/(2p)$ and ignoring the terms with a^4 or f^2, the approximate solution for ΔT_2 at the boundary of the hot wire is

$$\Delta T_2(a,t) = \frac{q}{4\pi\lambda_2}\ln\frac{4\alpha_2 t}{a^2C} - \frac{qBt}{4\pi\lambda_2} - \frac{qa^2B}{8\pi\lambda_2\alpha_2}\ln\frac{4\alpha_2 t}{a^2C} + \frac{qa^2}{8\pi\lambda_2\alpha_2 t}\ln\frac{4\alpha_2 t}{a^2C} + \frac{qfa^2}{16\pi\lambda_2}\left[\ln^2\left(\frac{4\alpha_2 t}{a^2C}\right) - \frac{\pi^2}{6}\right] \tag{A.35}$$

If the finite radius of the hot wire is not considered, the model changes to

$$\frac{\partial^2\Delta T_2}{\partial r^2} + \frac{1}{r}\frac{\partial\Delta T_2}{\partial r} - \frac{1}{\alpha_2}\frac{\partial\Delta T_2}{\partial t} = f\,\Delta T_2 \tag{A.36}$$

$$r \to 0, \qquad -r\frac{\partial\Delta T_2}{\partial r} = \frac{q}{2\pi\lambda_2} \tag{A.37}$$

$$r \to \infty, \qquad \Delta T_2 = 0 \tag{A.38}$$

so that after Laplace transformation

$$\frac{\partial^2\Delta\bar{T}_2}{\partial r^2} + \frac{1}{r}\frac{\partial\Delta\bar{T}_2}{\partial r} = \frac{p+B}{\alpha_2}\Delta\bar{T}_2 \tag{A.39}$$

$$r \to 0, \qquad -r\frac{\partial\Delta\bar{T}_2}{\partial r^2} = \frac{q}{2\pi\lambda_2} \tag{A.40}$$

$$r \to \infty, \qquad \Delta\bar{T}_2 = 0 \tag{A.41}$$

where

$$B = \frac{16Kn^2\sigma T_0^3}{\lambda_2} \tag{A.42}$$

The solution for this set of equations is

$$\Delta\bar{T}_2 = c_1 I_0(q_2 r) + c_2 K_0(q_2 r) \tag{A.43}$$

where $q_2 = \sqrt{(p+B)/\alpha_2} = \sqrt{p/\alpha_2 + f} \approx q_2'[1 + f/(2q_2')^2]$, $q_2' = \sqrt{p/\alpha_2}$, and $f = B/\alpha_2$. With the boundary conditions the two constants of the general solution, i.e., $c_1 = 0$ and $c_2 = q/(2\pi\lambda_2 p)$, can now be obtained so that, after using the Bessel function approximations, the solution of $\Delta\bar{T}_2$ results,

$$\Delta\bar{T}_2 = \frac{q}{2\pi\lambda_2 p}\left[-\ln\left(\frac{1}{2}Cq_2 r\right) - \frac{q_2^2 r^2}{4}\ln\left(\frac{1}{2}Cq_2 r\right) + \frac{q_2^2 r^2}{4}\right] \tag{A.44}$$

or the approximate solution,

$$\Delta T_2 = \frac{q}{4\pi\lambda_2}\ln\frac{4\alpha_2 t}{a^2 C}\left(1 + \frac{Ba^2}{4k_2}\right) - \frac{qBt}{4\pi\lambda_2} + \frac{qBa^2}{16\pi\lambda_2\alpha_2} + O\left(\frac{a^2}{\alpha_2 t}, B^2t^2\right) \tag{A.45}$$

This equation is identical to the one obtained by Nieto de Castro et al. [7]. It should be noted, however, that in this case the radiant energy emitted from the wire and the energy absorbed by the test medium and the hot wire have been ignored.

As stated, what is dominant to the problem is the energy emitted by the fluid. To compare the difference between Eq. (A.35) and Eq. (A.45),

Table AI. Thermal Conductivity and Thermal Diffusivity Values Obtained by Utilizing the Two Radiation Correction Approximations Applied to Data for Run ID Nos. P10_50A3 to P10_50D4

T (K)	q ($W \cdot m^{-1}$)	λ_1 ($W \cdot m^{-1} \cdot K^{-1}$)	$\alpha_1 \times 10^8$ ($m^2 \cdot s^{-1}$)	λ_2 ($W \cdot m^{-1} \cdot K^{-1}$)	$\alpha_2 \times 10^8$ ($m^2 \cdot s^{-1}$)	B (s^{-1})
375.96		**0.10479**	**6.975**	**0.10478**	**6.977**	
376.86	0.15802	0.10468	8.201	0.10467	8.199	0.025
376.88	0.15803	0.10487	8.452	0.10486	8.450	0.025
377.22	0.21478	0.10492	8.066	0.10491	8.064	0.025
377.23	0.21500	0.10482	7.946	0.10481	7.944	0.025
377.59	0.28209	0.10492	7.308	0.10491	7.306	0.025
377.60	0.28036	0.10478	7.566	0.10477	7.564	0.028
377.92	0.35441	0.10480	7.537	0.10478	7.535	0.028
377.93	0.35452	0.10495	7.746	0.10492	7.744	0.025

corrections of thermal radiation were made for measurements at 376 K and 34 MPa at different powers using both expressions. The deviation in the corrected temperature rise from the corresponding linear best fits for the measurement P1050A4 (Table II) is shown in Fig. 5 with the resulting thermal conductivity and thermal diffusivity, before and after adjustments for the influence of χ and the zero-time bridge temperature difference, listed in Table AI, where 1 and 2 denote the corrections applied to the data by Eqs. (A.35) and (A.45), respectively. From Fig. 5 and Table AI can be concluded that the difference between the use of these two expressions can be ignored ($\leqslant 0.01$ and $\leqslant 0.03\%$ for thermal conductivity and thermal diffusivity, respectively).

ACKNOWLEDGMENT

This work was performed under a program of studies funded by the Natural Sciences and Engineering Research Council of Canada under NSERC OPG 8859.

REFERENCES

1. N. B. Vargaftik, *Handbook of Physical Properties of Liquid and Gases*, 2nd ed. (Hemisphere, Washington, DC, New York and London, 1983), pp. 259–260.
2. I. T. Carmichael, J. Jacobs, and B. H. Sage, *J. Chem. Eng. Data* **14**:31 (1969).
3. A. M. F. Palavra, W. A. Wakeham, and M. Zalaf, *Int. J. Thermophys.* **8**:305 (1987).
4. H. S. Carslaw and J. G. Jaeger, *Conduction of Heat in Solids*, 2nd ed. (Clarendon Press, Oxford, 1959), pp. 339–341.
5. J. J. Healy, J. J. de Groot, and J. Kestin, *Physica C* **82**:393 (1976).
6. C. A. Nieto de Castro, R. A. Perkins, and H. M. Roder, *Int. J. Thermophys.* **12**:985 (1991).
7. C. A. Nieto de Castro, S. F. Y. Li, G. C. Maitland, and W. A. Wakeham, *Int. J. Thermophys.* **4**:311 (1983).
8. R. A. Perkins, H. M. Roder, and C. A. Nieto de Castro, *J. Res. Nad. Inst. Stand. Technol.* **96**:247 (1991).
9. J. Menashe and W. A. Wakeham, *Int. J. Heat Mass Transfer* **25**:661 (1982).
10. H. M. Roder, R. A. Perkins, and C. A. Nieto de Castro, *Int. J. Thermophys.* **10**:1141 (1989).
11. L. Sun, J. E. S. Venart, and R. C. Prasad, *Int. J. Thermophys.* **23**:357 (2002).
12. L. Sun, Doctoral dissertation (University of New Brunswick, Fredericton, 2001).
13. E. F. Buyukicer, J. E. S. Venart, and R. C. Prasad, *High Temp. High Press.* **18**:55 (1986).
14. R. Span, *Multiparameter Equations of State—Accurate Source of Thermodynamic Property Data* (Springer, Berlin/Heidelberg/New York, 2000).
15. E. W. Lemmon, A. P. Peskin, M. O. McLinden, and D. G. Friend, *NIST Standard and Reference Database 12*, Version 5.0 (2000).
16. G. H. Wang, J. E. S. Venart, and R. C. Prasad, *Proc. 11th Symp. Thermophys. Prop.*, Boulder, CO, June 23–27 (1991).
17. J. Menashe and W. A. Wakeham, *Ber. Bunsenges. Phys. Chem.* **85**:340 (1981).